



Parametrically Excited Vibration in Rolling Element Bearings

R. Srinath¹; A. Sarkar²; A. S. Sekhar³

^{1,2,3} Indian Institute of Technology Madras, India, 600036

ABSTRACT

A defect-free rolling element bearing has a varying stiffness. The variation of stiffness depends on number of rolling elements, their configuration and cage frequency. The time-varying characteristics of the stiffness results in a parametric excitation. This may lead to instability which is manifested as high vibration levels. An FEM simulation is performed to evaluate stiffness in each configuration of rolling elements and is used to study the variation of direct stiffness and cross coupled stiffness. The obtained stiffness variation is expanded into a Fourier series to form the equation of motion for the bearing vibration. As the stiffness varies with cage frequency, stiffness term in the equation of motion is periodic with parametric excitation. Hence, the equation of motion is a 2-DOF coupled Mathieu equation. Based on Mathieu parameters and cage frequency there exists unstable rpm ranges for a particular bearing. Floquet theory is employed to find out the stable and unstable regions. This involves finding out maximum Floquet exponent using Monodromy matrix. The results obtained through Floquet theory are in agreement with the numerical solution of the governing equations.

Keywords: Vibration, stability I-INCE Classification of Subjects Number(s): 11.1.1, 40, 41.1, 21.7

1. INTRODUCTION

Rolling element bearings are important components of any rotating machinery and one of the common sources of machine noise and vibration. Due to its wide industrial applications, investigation of the dynamic characteristics of such machine elements has received a considerable attention in the research community. The principal complication associated with the dynamics of such bearings arises due to the parametric excitation. As the rolling element rolls between the inner and the outer race, the effective stiffness of the bearing assembly changes periodically with the change in configuration of the rolling elements. This varying stiffness induces a parametric excitation.

Investigation of dynamics effects of varying compliance using motion simulation was done by Walters [1]. The model developed was generic and did not capture the effect of geometry of the rolling elements. As an improvement to this work, Gupta [2] developed a dynamic model for both ball and cylindrical roller bearings. In these works, a non-linear Hertzian contact stiffness was assumed between the rolling element and the cage material. Estimation of the stiffness parameters in these works remained challenging. Static stiffness was estimated by Shimizu *et. al.* [3]- [5]. The work reported that the overall stiffness changes with different positions of the rolling elements. This results in change in natural frequency of the system in various configurations over a cycle of rotation. Their work clearly highlights the importance of parametric excitation in roller bearings. A classical method of solution for such parametrically excited system is based on the Floquet theory [6]. Zhang *et. al.* [7] applied Floquet theory in studying the dynamic characteristics of rotor-bearing system.

The objective of the present work is to investigate the dynamic characteristics of a rolling element bearing independent of the rotor system. The parametric excitation is known to be dependent on the operating speed. Also, it is well-known that parametric excitation induces stable (decaying) and unstable (growing) vibration. Thus, the aim of the present work is to identify the stable and unstable dynamic characteristics of a bearing as a function of its operating speed. Governing equations of motion for such system is derived and recast into a 2-Dof Mathieu equation. Floquet theory based analysis is employed for determining the stability for a given set of parameters.

¹srinath.ramagiri@gmail.com

²asarkar@iitm.ac.in

³as_sekhar@iitm.ac.in

2. FORMULATION

A typical rolling element bearing has inner race, outer race, rolling elements and cage as its basic components as shown in Fig.1(a). The inner and outer race are assumed to be rigidly connected to separate machine elements. Thus, the compliance of the bearing assembly is primarily derived due to the flexibility of the rolling elements. Our primary objective is to develop an equivalent model of the bearing system by replacing the actual rolling elements with lumped springs as shown in Fig. 1(b). The motion of this equivalent bearing assembly remains in the plane. Thus, with the assumption of rigidity of the inner and outer race as described above, Fig.1(b) can be replaced with Fig.1(c) and 2-Dof equation of the form

$$[M] \begin{Bmatrix} \ddot{x} \\ \ddot{y} \end{Bmatrix} + [K] \begin{Bmatrix} x \\ y \end{Bmatrix} = 0 \quad (1)$$

is to be developed.

At a general configuration of the bearing assembly, the rolling elements are asymmetrically positioned as shown in Fig.(2) with Config-2. Thus, a x-directional force leads to a y-direction displacement and *vice versa*. This leads to a direct stiffness (force and displacement along the same direction) and a coupled stiffness (force and displacement along orthogonal directions). The direct and coupled stiffness parameters form the diagonal and non-diagonal entries of the stiffness matrix K in Eq. (1), respectively.

As discussed above, the load transfer between the inner and the outer race takes place through the rolling elements. However, not all the rolling elements share the load equally. The load sharing between the elements is governed by the load zone effects which depends on clearance. In the present work, zero clearance is assumed which leads to a load zone of 180° as shown in Fig.1(a). Both the direct and the coupled stiffness of the bearing assembly in a particular configuration is decided by the number of rolling elements in the load zone. For a bearing running at its operating speed, the number of rolling elements and their configuration within the load zone changes with time. This in turn leads to a varying stiffness or parametric excitation. Thus, Eq. (1) is modified as

$$[M] \begin{Bmatrix} \ddot{x} \\ \ddot{y} \end{Bmatrix} + [K(t)] \begin{Bmatrix} x \\ y \end{Bmatrix} = 0. \quad (2)$$

In the following subsection, we determine the values of mass and stiffness matrices for a particular industrial bearing.

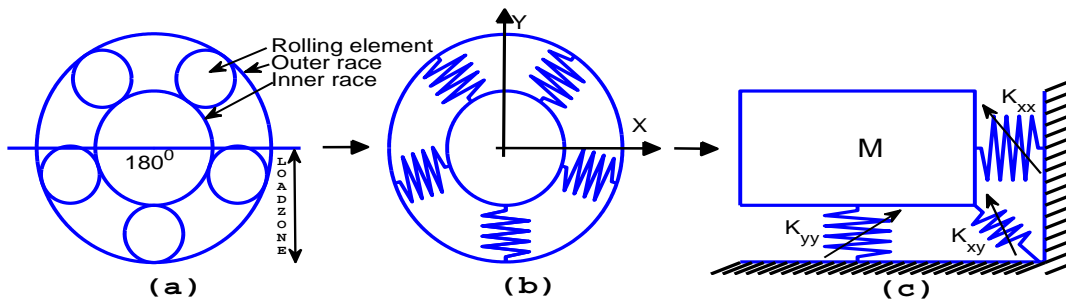


Figure 1 – (a)Bearing with rolling elements, (b)Bearing with lumped springs, (c)Equivalent Spring mass system.

3. DYNAMICS OF A BEARING

The details of a bearing with five rolling elements are presented in Table(1). Finite element simulations are performed in ANSYS 13.0 software environment to evaluate stiffness of a rolling element. A single rolling element is modelled in ANSYS 13.0. Vertical load is applied that compresses rolling element. Ratio of amount of load applied to the deflection of rolling element gives the stiffness of single rolling element. The stiffness is estimated as $4 \times 10^8 \text{ N/m}$. The equivalent springs with stiffness estimated from FEM are considered for analysis as shown in Fig.1(b). To start with, Config-1 in Fig.2 is used. The configuration is rotated clock wise to calculate the stiffness values. A constant vertical deflection is given to the inner race at each configuration. The springs that undergo compression are tracked, vertical and horizontal reactions of these compressed springs are evaluated. The ratio of sum of vertical reaction and the vertical displacement is direct stiffness, the ratio of sum of horizontal reaction and the vertical deflection is cross coupled stiffness. Same procedure is followed with different configuration of rolling elements. As different configuration of rolling element result in different magnitude of direct and cross coupled stiffness, a variation of stiffness is seen with respect to

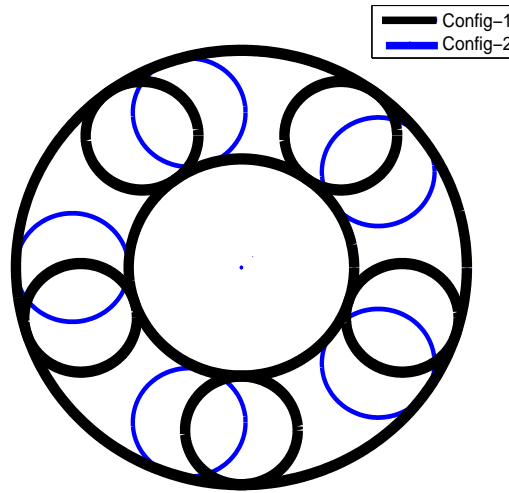


Figure 2 – Symmetric and Unsymmetrical configuration .

rolling element configuration change. Here a 5 rolling element bearing is considered, hence is sufficient if the stiffness variation is evaluated over 72° because the same variation gets repeated 5 times over 360° . The direct and cross coupled stiffness at each angular displacement are evaluated and are plotted with respect to angular displacement as shown in Fig.3 and 5.

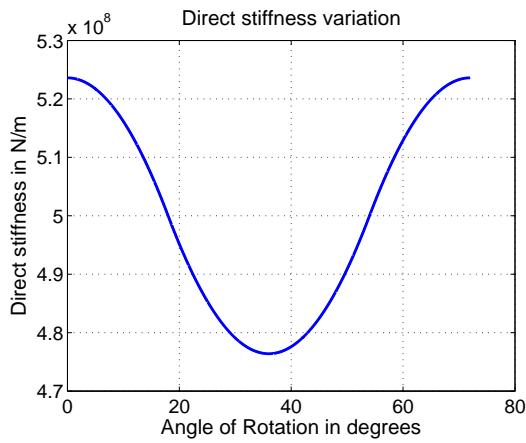


Figure 3 – Direct stiffness variation

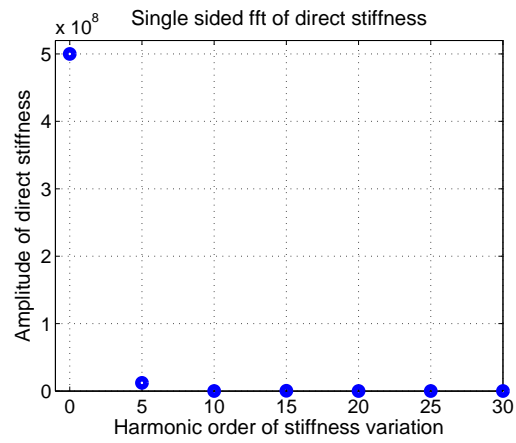


Figure 4 – Coupled stiffness variation

The variation of stiffness shown in Fig.3 and 5 are decomposed into its harmonics and are presented in Fig.4 and 6. Using the magnitudes of different harmonics and their harmonic numbers it is easy to represent the variation of stiffness in terms of sinusoids which are functions of time and speed of operation. For example the variation shown in Fig.3 contains a mean stiffness value about which there is some variation. The corresponding mean value is read from Fig.4 at zero harmonic number. The amplitude of the variation is the value on $y - axis$ at a harmonic number of 5. These two values can be used to approximately represent the direct stiffness variation shown in Fig.3 as $K_{yy} + K\cos(5\omega t)$ which is stiffness in vertical direction. Similar equation results if the stiffness in horizontal direction is evaluated but there will be a 90° difference in angle. A 90° rotated configuration is shown with Config-1 in Fig.2. Following the same procedure, cross coupled stiffness equation is written. The dominant harmonics are chosen for analysis and are tabulated in Table1. The equation of motion can be written using Newton’s second law as

$$m \frac{d^2x}{dt^2} + [K_{xx} - K\sin(n\omega t)]x + [K_{xy}\cos(n\omega t)]y = 0 \tag{3}$$

$$m \frac{d^2y}{dt^2} + [K_{yy} + K\cos(n\omega t)]y + [K_{yx}\sin(n\omega t)]x = 0 \tag{4}$$

where m is the mass of inner race, K_{xx} and K_{yy} are the mean value of stiffness variation along x and y directions respectively. K is the magnitude of stiffness variation along x and y direction. Also K_{xy} and K_{yx} are the magnitudes of cross coupled stiffness variation. Clearly the equation of motion is linear, coupled,

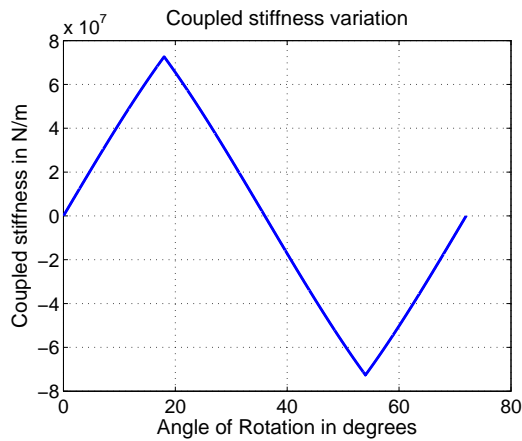


Figure 5 – Direct stiffness frequency plot

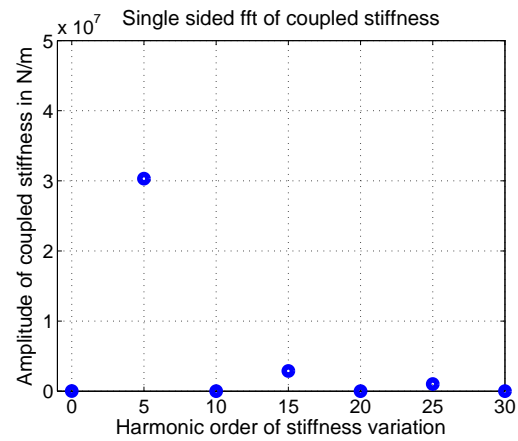


Figure 6 – Coupled stiffness frequency plot

un-damped and parametric in nature. For analysis Eq.(3) and Eq.(4) can be written in non-dimensional form as shown below

$$\frac{d^2x^*}{dt^{*2}} + [K_{xx}^* - 2K^* \sin(2t^*)]x^* + [2K_{xy}^* \sin(2t^*)]y^* = 0 \quad (5)$$

$$\frac{d^2y^*}{dt^{*2}} + [K_{yy}^* + 2K^* \cos(2t^*)]y^* + [2K_{yx}^* \cos(2t^*)]x^* = 0 \quad (6)$$

Where $n\omega t = 2t^*$; $K_{xx}^* = \frac{4K_{xx}}{mn^2\omega^2}$; $K_{yy}^* = \frac{4K_{yy}}{mn^2\omega^2}$; $2K^* = \frac{4K}{mn^2\omega^2}$; $2K_{xy}^* = \frac{4K_{xy}}{mn^2\omega^2}$; $2K_{yx}^* = \frac{4K_{yx}}{mn^2\omega^2}$

The equation of motion is two dimensional coupled Mathieu equation. For a given geometry of bearing and

Table 1 – Stiffness values and Bearing data (5 rolling elements).

Attributes	Values	Stiffness	Mean value (N/m)	1 st harmonic (N/m)
Bore dia	20 mm	K_{xx}	5×10^8	24×10^6
Outer dia	47 mm	K_{yy}	5×10^8	24×10^6
Width	14 mm	K_{xy} or K_{yx}	0	60×10^6

its material the stiffness terms in the equation of motion are fixed. The only parameter that changes is the operating speed. Since the system is parametric in nature there may be operating speeds at which the free response may grow or decay. The system is said to be unstable in the former and stable in latter case. The closed form solution is not possible in this case hence a qualitative analysis is done to predict the stability.

4. INSTABILITY RANGE PREDICTION

A general theory for stability analysis is given in this section. The equation of motion derived in the previous section is a special case of Hill's equation. Stability of such equation can be studied using Floquet theory. Floquet theory for a single Dof Hill's equation is discussed in brief. A detailed analysis is given in Nayfeh [6].

4.1 Floquet theory applied to Hill's equation

Hill's equation is of the form

$$\frac{d^2r}{dt^2} + b(t)r = 0, b(t) = b(t+T) \quad (7)$$

where r and b are scalar valued functions, b is periodic with period T . Equation 7 can be written in first order form using state space method by assuming $R = \begin{Bmatrix} r_1 \\ r_2 \end{Bmatrix}$, $[B(t)] = \begin{bmatrix} 0 & 0 \\ -b(t) & 0 \end{bmatrix}$

where $r_1 = r$ and $r_2 = \frac{dr}{dt}$ and the Eq.7 can be written as

$$\dot{R} + [B(t)]R = 0 \quad (8)$$

A fundamental solution matrix is assumed. A 2×2 unit matrix ($I_{2 \times 2}$) can be a fundamental solution matrix for Eq.(8). Eq.(8) is solved by taking each column of $I_{2 \times 2}$ as initial condition. Each initial conditions vector gives another solution vector at the end of time T. A 2×2 matrix is formed using all the solution vectors evaluated at the end of time T. This solution matrix is called Monodromy matrix and is represented by C. The stability of the response depends on the eigenvalues of C as given below

- If magnitude of maximum eigenvalue of C is more than 1 then the system is unstable.
- If magnitude of maximum eigenvalue of C is less than 1 then the system is stable.
- If magnitude of maximum eigenvalue of C is equal to 1 then the response of the system is periodic with period T or 2T.

The eigenvalues of matrix C are called Floquet Exponents. Mathieu equation is a special case of Hill's equation and is given as $\ddot{x} + (\delta - 2\epsilon\cos(2t))x = 0$ where δ and ϵ are called as parameters of Mathieu equation. Using Floquet theory the stability plot for a Mathieu equation is drawn between ϵ and δ as given in [6].

4.2 Floquet theory applied to bearing equation of motion

Bearing equation of motion in non-dimensional form as shown in Eq.(5) and (6) can be written as

$$\begin{bmatrix} 1 & 0 \\ 0 & 1 \end{bmatrix} \begin{Bmatrix} \ddot{x}^* \\ \ddot{y}^* \end{Bmatrix} + \begin{bmatrix} K_{xx}^* - 2K^* \sin(2t^*) & 2K_{xy}^* \cos(2t^*) \\ 2K_{yx}^* \sin(2t^*) & K_{yy}^* + 2K^* \cos(2t^*) \end{bmatrix} \begin{Bmatrix} x^* \\ y^* \end{Bmatrix} = 0 \tag{9}$$

$$m \frac{d^2x}{dt^2} + \hat{C} \frac{dx}{dt} + [K_{xx} - K \sin(n\omega t)]x + [K_{xy} \cos(n\omega t)]y = 0 \tag{10}$$

$$m \frac{d^2y}{dt^2} + \hat{C} \frac{dy}{dt} + [K_{yy} + K \cos(n\omega t)]y + [K_{yx} \sin(n\omega t)]x = 0 \tag{11}$$

For computational ease unit mass of inner race is assumed. The stiffness matrix is periodic with period π . The parameters K_{xx}^* , K_{yy}^* , K_{xy}^* , K_{yx}^* and K^* are functions of stiffness of single rolling element and angular velocity ω . At each ω the values of these parameters are different. The changing non-dimensional parameters in Eq.(9) are taken into account for the analysis. Eq.(9) is two dimensional Mathieu equation, hence a 4×4 fundamental solution matrix is required which is $I_{4 \times 4}$. Eq.(9) is solved numerically up to $t^* = \pi$ by taking each column of fundamental solution matrix as initial condition. The solution vector at $t^* = \pi$ corresponding to each initial condition is used to form the Monodromy matrix C . Eigenvalues of C are computed. Magnitude of these eigenvalues are obtained. The maximum of these absolute values computed is used for stability analysis based on the conditions presented in previous section. For a bearing once installed, the only varying parameter is the speed of operation. Angular velocity ω does not appear in Eq.(9) explicitly. The non-dimensional parameters in Eq.(9) changes with ω . Here the stability plot is drawn between Floquet exponent and angular velocity of inner. The stability plot is presented in Fig.7.

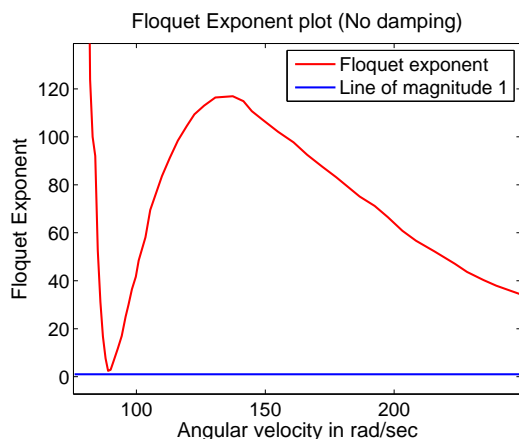


Figure 7 – Floquet Exponents plot with zero damping.

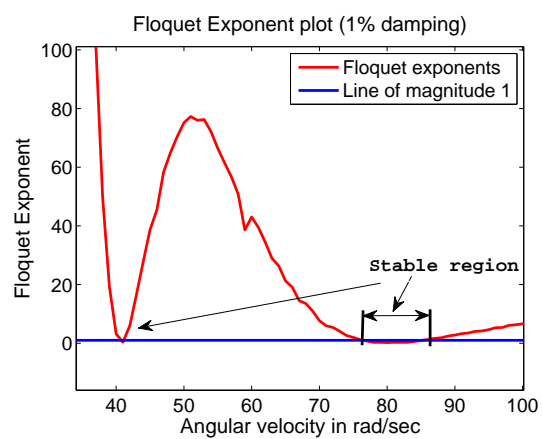


Figure 8 – Floquet Exponents plot with 1% damping.

Clearly Fig.7 shows that an un-damped rolling element bearing is always unstable for any speed of operation. Specifically, observing the Floquet exponents, it can be concluded that the bearing response goes asymptotically stable as the operating speed increases. This counter-intuitive inference is attributed to the un-damped model considered.

The same analysis is refined by including damping effects. Eq.(10) and (11) show the equation of motion with damping in dimensional form. \hat{C} is the damping present in the system. Fig.8 and 9 are plotted with

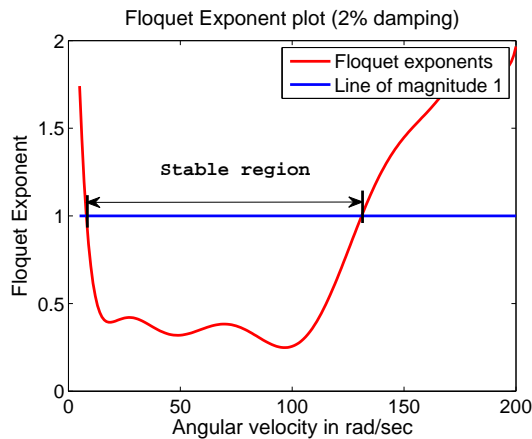


Figure 9 – Floquet Exponents plot with 2% damping.

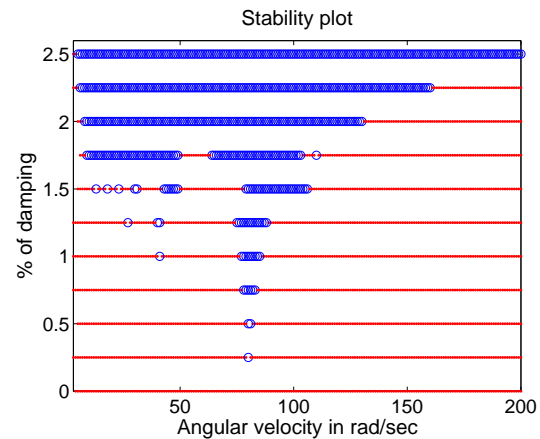


Figure 10 – Stability zones of angular velocity for different values of damping.

1%, 2% of C_c (the critical damping) respectively. The magnitude of Floquet exponent over unity dictates the severity of the instability. With the addition of damping, stable angular velocities appear that correspond to a relatively low value of Floquet exponent. Fig.8 shows two such stable speed ranges with an intermediate unstable range. This unstable region gets stabilised for the case of 2 % damping as shown in Fig.9. Extending this analysis, stable and unstable angular velocities are demarcated for different values of damping. These results are presented in Fig.10. Circle points are stable points and dots represent unstable points. Different stable and unstable velocity intervals are observed for different values of damping. With increase in damping, the intermediate unstable speed ranges diminish in size and finally are consumed within the neighbouring stable ranges. If the amount of damping increases more than 2.5%, then it is observed that the system is stable within the speed 0-200 rad/s.

5. CONCLUSIONS

In the present work, a 2-dimensional equation of motion is formulated for a rolling element bearing. The model assumes the inner and outer race to be rigid but accounts for the compliance of the rolling elements. The stiffness of each rolling element is estimated from FEA simulation. The obtained stiffness is used to calculate the direct and coupled stiffness variation. Only the dominant harmonic in stiffness variation is considered. The governing equation of motion of the bearing assembly is thus derived in the form of a coupled 2-Dof Mathieu equation. Using Floquet theory, stability analysis is carried out for different operating speeds of the bearing. It is observed that the undamped system is unstable at all operation speeds. With little amount of damping, intermittent stable regions are predicted together with unstable regions. However, inclusion of a realistic value of damping results in a continuous stable range of operating speed.

REFERENCES

1. Walters C. T., The dynamics of ball bearings. ASME Journal of Lubrication Technology. 1971;93:1–10.
2. Gupta P. K., Dynamics of rolling element bearings Parts I-IV. ASME Journal of Lubrication Technology. 1979;101:293–326.
3. Shimizu H. and Tamura H., Vibration of rotor based on ball bearing. 1st report: static stiffness of ball bearings. Bull. Jap. Soc. Mech. Engrs. 1966;9:524–536.
4. Shimizu H. and Tamura H., Vibration of rotor based on ball bearing. 2rd report: static stiffness of a ball bearings containing a large number of balls. Bull. Jap. Soc. Mech. Engrs. 1967;10:763–775.
5. Shimizu H. and Tamura H., Vibration of rotor based on ball bearing. 3rd report: static stiffness of a ball bearings containing a large number of balls. Bull. Jap. Soc. Mech. Engrs. 1968;11:825–837.
6. Nayfeh A. H and Mook D. T., Nonlinear Oscillations. John Wiley and Sons, New York, 1995.
7. Zhang X, Han Q, Peng Z, Chu F., Stability analysis of a rotor-bearing system with time-varying bearing stiffness due to finite number of balls and unbalanced force. Journal of Sound and Vibration 2009;325:145-160.